Biochimica et Biophysica Acta 1842 (2014) 2306–2317

Contents lists available at ScienceDirect

Biochimica et Biophysica Acta

journal homepage: www.elsevier.com/locate/bbadis

A novel proteolysis-resistant cyclic helix B peptide ameliorates kidney ischemia reperfusion injury

Cheng Yang [a,b,1], Zhongliang Xu [c,1], Zitong Zhao [a,b,1], Long Li [a,b], Tian Zhao [a,b], Dian Peng [c], Ming Xu [a,b], Ruiming Rong [a,b,d,*], Ya-Qiu Long [c,**], Tongyu Zhu [a,b,e,***]

[a] Department of Urology, Zhongshan Hospital, Fudan University, Shanghai, China
[b] Shanghai Key Laboratory of Organ Transplantation, Shanghai, China
[c] CAS Key Laboratory of Receptor Research, Shanghai Institute of Materia Medica, Chinese Academy of Sciences, Shanghai, China
[d] Department of Transfusion, Zhongshan Hospital, Fudan University, Shanghai, China
[e] Qingpu Branch Zhongshan Hospital, Fudan University, Shanghai, China

ARTICLE INFO

Article history:
Received 12 April 2014
Received in revised form 14 August 2014
Accepted 2 September 2014
Available online 9 September 2014

Keywords:
Cyclic helix B peptide
Metabolic stability
Kidney ischemia reperfusion injury
Autophagy
Apoptosis
Inflammation

ABSTRACT

Helix B surface peptide (HBSP), derived from erythropoietin, displays powerful tissue protection during kidney ischemia reperfusion (IR) injury without erythropoietic side effects. We employed cyclization strategy for the first time, and synthesized thioether-cyclized helix B peptide (CHBP) to improve metabolic stability and renoprotective effect. LC–MS/MS analysis was adopted to examine the stability of CHBP in vitro and in vivo. The renoprotective effect of CHBP in terms of renal function, apoptosis, inflammation, extracellular matrix deposition, and histological injury was also detected in vivo and in vitro. Antibody array and western blot were performed to analyze the signal pathway of involvement by CHBP in the IR model and renal tubular epithelial cells. In this study, thioether-cyclized peptide was significantly stable in vivo and in vitro. One dose of 8 nmol/kg CHBP administered intraperitoneally at the onset of reperfusion improved renal protection compared with three doses of 8 nmol/kg linear HBSP in a 48 h murine IR model. In a one-week model, the one dose CHBP-treated group exhibited remarkably improved renal function over the IR group, and attenuated kidney injury, including reduced inflammation and apoptosis. Interestingly, we found that the phosphorylation of autophagy protein mTORC1 was dramatically reduced upon CHBP treatment. We also demonstrated that CHBP induced autophagy via inhibition of mTORC1 and activation of mTORC2, leading to renoprotective effects on IR. Our results indicate that the novel metabolically stable CHBP is a promising therapeutic medicine for kidney IR injury treatment.

1. Introduction

Erythropoietin (EPO) is an endogenous protein that exerts tissue-protective effects for a wide range of organs, but it causes unfavorable side effects because of the very high dose requirement necessary to achieve tissue protection [1]. Helix B surface peptide (HBSP), an 11-amino acid sequence derived from the aqueous surface of the helix B domain of EPO, was recently shown to exert powerful tissue-protective function in various organs subjected to ischemia reperfusion (IR) injury by inhibiting inflammation and apoptosis [2,3]. However, the 2-minute plasma half-life of HBSP restricts its application in vivo [2]. Therefore, structurally optimized transformation of HBSP is required. Similar to EPO, pyroglutamate helix B surface peptide (pHBSP, also known as ARA290) was found to attenuate renal IR injury [4]. Interestingly, pHBSP does not always share the same mechanism with EPO [3]. Although pHBSP also has a plasma half-life of only 2 min [5], these results indicated that the artificial analogs of HBSP produce the same or even better effects. Cyclization is an efficient approach to stabilize the secondary structure of the linear peptide and improve metabolic stability and potency [6–8]. Therefore, based on the amino acid sequence of HBSP, we designed and synthesized a series of conformationally constrained helix B peptides with the goal of increased resistance to proteolytic degradation, improving renoprotective potency, and decreasing administrative time and dose.

Optimizing kidney preservation is a primary issue in transplantation, particularly relative to new donor sources, such as expanded criteria

* Correspondence to: R. Rong, Department of Urology and Department of Transfusion, Zhongshan Hospital, Fudan University; Shanghai Key Laboratory of Organ Transplantation, 180 Fenglin Road, Shanghai 200032, China. Tel.: +86 21 64041990; fax: +86 21 64037269.
** Correspondence to: Y.-Q. Long, CAS Key Laboratory of Receptor Research, Shanghai Institute of Materia Medica, Chinese Academy of Sciences, 555 Zuchongzhi Road, Shanghai 201203, China. Tel.: +86 21 50806876; fax: +86 21 50807088.
*** Correspondence to: T. Zhu, Department of Urology, Zhongshan Hospital, Fudan University; Shanghai Key Laboratory of Organ Transplantation, 180 Fenglin Road, Shanghai 200032, China; Qingpu Branch Zhongshan Hospital, Fudan University, 1158 Gongyuan Road East, Shanghai 201700, China. Tel.: +86 21 64037287; fax: +86 21 64037269.
E-mail addresses: rong.ruiming@zs-hospital.sh.cn (R. Rong), yqlong@mail.shcnc.ac.cn (Y.-Q. Long), tyzhu_dr@163.com, tyzhu@fudan.edu.cn (T. Zhu).
[1] These authors contributed equally to this article.

http://dx.doi.org/10.1016/j.bbadis.2014.09.001
0925-4439/

donors and donation after cardiac death. Kidneys from these donors are highly sensitive to IR injury, which is a major cause of delayed graft function and affects both short- and long-term graft survivals. However, no potent therapy is confirmed thus far. Overwhelming evidence has suggested that kidney IR injury is an inflammatory disease mediated by innate and adaptive immunity [9]. Apoptosis, inflammation [10], and complement cascades [11] are all initiated by kidney IR injury. Imbalance of tissue-protective regulatory T (Treg) cells and tissue-destructive T helper 17 (Th17) cells, caused by the imbalance of pro- and anti-inflammatory cytokines in the milieu, has also been confirmed in injured allografts resulting from IR [12].

Autophagy, an evolutionarily conserved process of lysosome-dependent turnover of damaged proteins and organelles, is present in normal kidneys and upregulated in response to stress, such as IR injury [13]. Autophagy is believed to exert a beneficial role in IR injury as rapamycin, an mTOR inhibitor and potent inducer of autophagy, ameliorates tubular injury and reduces renal dysfunction [14]. Many recent findings suggest that glucose deprivation during IR triggers autophagy via the activation of AMP-dependent protein kinase (AMPK) and inhibition of mTOR in the hearts [15]. In addition, the PI3K–Akt signaling pathway has also been proven to play an important role in autophagy [13].

In the current paper, we describe the design and synthesis of a novel cyclic analog of HBSP, designated as CHBP. Furthermore, we demonstrated that CHBP exhibited better metabolic stability and renoprotective effects than its linear counterpart. Given that HBSP has been elucidated to protect the kidney from IR injury via PI3K/Akt signaling as well as signal transducer and activator of transcription (STAT) [3,16], we postulate that this novel CHBP might exert its renoprotective function by similar mechanisms. Moreover, we found that reduced apoptosis and inflammatory responses might be associated with IR-induced autophagy.

2. Materials and methods

2.1. Peptide synthesis

The synthetic procedure for the cyclized peptides (Fig. 1A) and additional details on the methods and circular dichroism (CD) measurements are provided in the Supplementary material.

2.2. Three different synthetic cyclopeptides

Thioether-cyclized peptide, CHBP: ESI-MS *m/z*: calculated 1416.7 $(M + H)^+$, found 1416.8; $t_R = 15.012$ min (10%–90% of solvent B in 30 min, purity 98.86%); $t_R = 25.123$ min (10%–90% of solvent C in 30 min, purity 98.44%).

(*R*)-Configured sulfoxide-cyclized peptide: ESI-MS *m/z*: calculated 1432.6 $(M + H)^+$, found 1432.7; $t_R = 14.011$ min (10%–90% of solvent B in 30 min, purity 99.33%); $t_R = 24.993$ min (10%–90% of solvent C in 30 min, purity 99.82%).

(*S*)-Configured sulfoxide-cyclized peptide: ESI-MS *m/z*: calculated 1432.6 $(M + H)^+$, found 1432.7; $t_R = 14.044$ min (10%–90% of solvent B in 30 min, purity 98.43%); $t_R = 25.025$ min (10%–90% of solvent C in 30 min, purity 99.00%).

2.3. Stability in the plasma and hepatocytes

The stabilities of CHBP and HBSP were detected using blank human plasma from healthy volunteers and hepatocyte solution (In Vitro Technologies, Victoria, Australia). Details are available in the Supplementary material.

2.4. In vivo metabolic stability

The metabolism of CHBP and HBSP was detected in vivo using Sprague–Dawley rats, which could supply sufficient blood samples for detection at successive time points in the same individual. Details are available in the Supplementary material.

2.5. Kidney IR injury

Male BALB/c mice (weighing 20–25 g) were obtained from Shanghai Slac Lab Animal, Co., Ltd., and bred in an experimental animal room of SPF grade. All animal procedures were performed according to the guidelines of the Care and Use of the Laboratory Animal Ethical Commission of Fudan University. The kidney IR model was established as previously described [3], and details are outlined in the Supplementary material.

To select an optimal peptide from the three cyclized peptides, mice were given a kidney IR injury and randomly divided into six groups ($n = 6$) according to different treatments: (1) IR group: PBS; (2) HBSP one dose group: one dose of 8 nmol/kg; (3) HBSP three dose group: three doses of 8 nmol/kg administered at the onset, 6 h, and 12 h post-reperfusion; (4) thioether-CHBP group: one dose of 8 nmol/kg; (5) (*R*)-sulfoxide-CHBP group: one dose of 8 nmol/kg; and (6) (*S*)-sulfoxide-CHBP group: one dose of 8 nmol/kg. All agents were intraperitoneally (i.p.) injected at the onset of reperfusion, except the third group. Animals were ethically sacrificed at 48 h post-reperfusion.

To evaluate the renoprotective effect and mechanism of CHBP, mice were randomly divided into two groups ($n = 36$): (1) IR group: IR injury with PBS i.p. injected; and (2) CHBP group: IR injury with one dose of 8 nmol/kg CHBP i.p. injected at the onset of reperfusion. Animals were ethically sacrificed at 6 h, 12 h, 24 h, 48 h, 5 d, and 7 d post-reperfusion ($n = 6$ for each time point). Whole blood and kidney samples were acquired and prepared for further examination as previously described [3].

2.6. Extracellular matrix deposition assay

The deposition of the extracellular matrix was evaluated by Sirius Red (collagen specific dye) staining, as previously described [10]. Details are available in the Supplementary material.

2.7. Histological assessment

Hematoxylin and eosin (H&E) staining was performed to assess histological injury. Details are available in the Supplementary material.

2.8. In situ end labeling (ISEL) apoptotic cells

ISEL apoptotic cells were detected using a TUNEL Apoptosis Detection Kit (Millipore, MA, USA). Details are available in the Supplementary material.

2.9. Immunohistochemistry

Immunohistochemical staining of myeloperoxidase (MPO) and cleaved caspase-3, which recognizes the 17 kDa active subunit, was performed on paraffin sections using a DAKO ChemMate EnVision Detection Kit (DAKO). Details are available in the Supplementary material.

2.10. Enzyme-linked immunosorbent assay (ELISA) of complement 3 (C3)

C3 was assayed in duplicate using sandwich ELISA (Quantikine Kit for Mice Complement 3 Immunoassay; GenWay, San Diego, CA, USA). The sample preparation and procedure were performed according to the manufacturer's instructions.

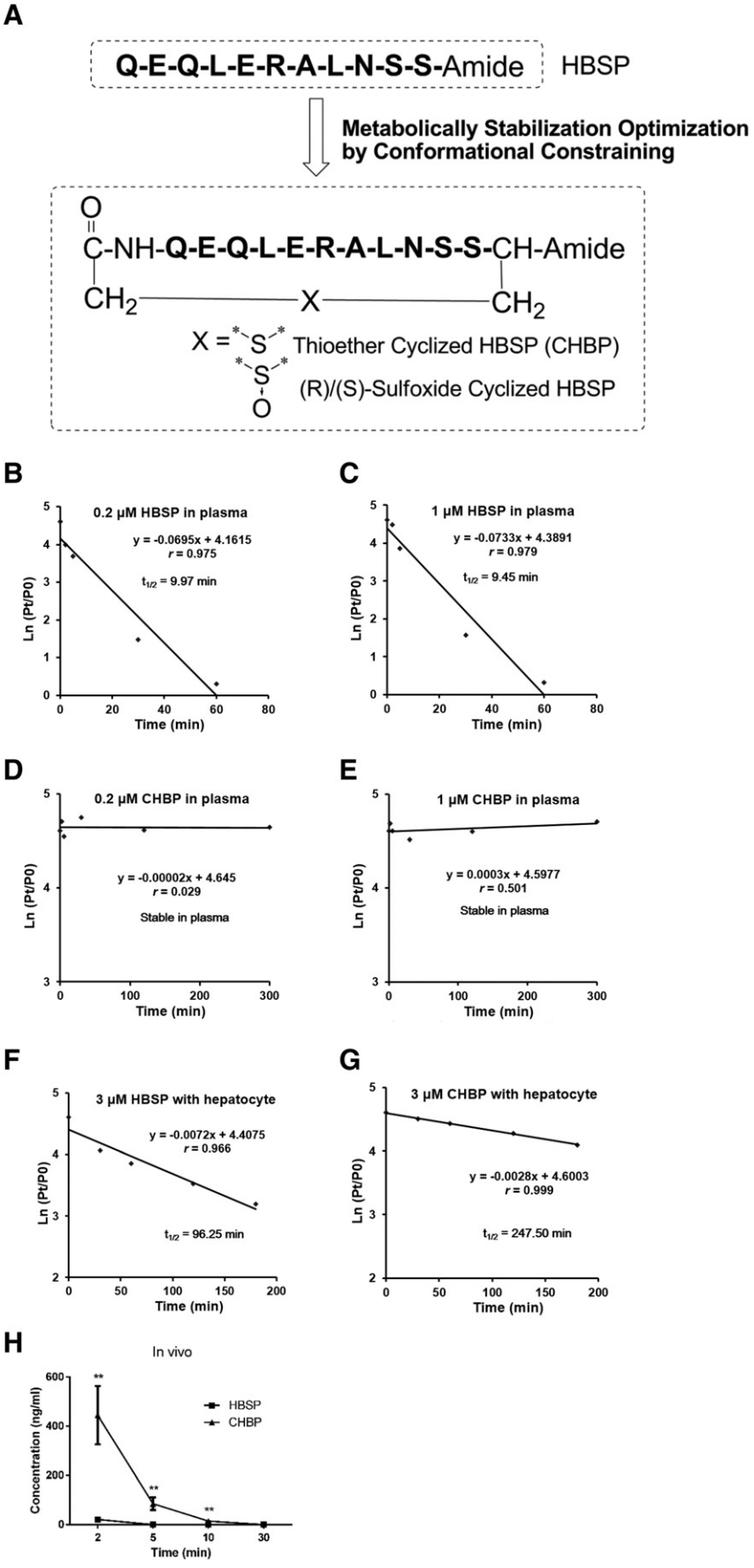

Fig. 1. Peptide synthesis and metabolic stability. Metabolically stabilized structural modification on the HBSP of EPO by thioether and sulfoxide cyclization (A). Thioether-CHBP remarkably improved stability in the human plasma and human hepatocytes in vitro (B–G), as well as in rats in vivo (H).

2.11. Real-time quantitative PCR (qPCR)

The mRNA expression of TNF-α, IL-6, IL-10, IL-17A, IL-17F, RORγt, and Foxp3 was measured by real-time qPCR. Details are available in the Supplementary material.

2.12. Tubular epithelial cell (TEC) stimulation and apoptosis detection

Mice renal proximal TECs were cultured and incubated with HBSP (1 μM) or CHBP (1 μM) for 12 h, and stimulated with 50 μM H_2O_2 (Sinopharm Chemical Reagent Co., Ltd., Shanghai, China) for 45 min. PBS was used as a positive control, and normal TEC without any stimulation was used as a negative control. After washing and changing the medium, the TEC was cultured for 24 h with PBS, HBSP, or CHBP. Cell apoptosis was detected by an Annexin V-FITC Apoptosis Detection Kit (Merck, Darmstadt, German) as mentioned previously [17]. The experiment was repeated at least three times.

2.13. Antibody array

A PathScan Intracellular Signaling Array Kit (Chemiluminescent Readout, Cell Signaling Technology) was used for the simultaneous detection of 18 phosphorylated or cleaved signaling proteins in the kidney. Details are available in the Supplementary material.

2.14. Western blot analysis

Membrane proteins were separated on SDS-polyacrylamide gels and transferred to polyvinylidene difluoride membranes. The membranes were blocked with 5% milk and incubated overnight with anti-beclin-1, anti-p-Akt (Ser473), anti-Akt, anti-p-mTOR (Ser2448), anti-p-mTOR (Ser2481), anti-mTOR, anti-p-p70S6K (Thr389), anti-p70S6K, anti-LC3, anti-raptor, anti-rictor (Cell Signaling, Beverly, MA, USA, 1:1000), and anti-β-actin (Abcam, Cambridge, UK, 1:10,000) antibodies. The results were analyzed as previously described [18].

2.15. Statistical analysis

Data are presented as mean ± standard deviation (SD). Statistical analysis (SPSS 18.0 software, SPSS Inc, Armonk, NY, USA) was performed with the two-tailed independent Student's *t*-test after the demonstration of homogeneity of variance with the F test or one-way ANOVA for more than two groups. The Scheffe test was used for post-hoc analysis. Statistical significance was set as $p < 0.05$.

3. Results

3.1. Thioether cyclization of HBSP remarkably improved the metabolic stability

Peptide cyclization provides an effective approach to tackle the problems of poor cell permeability, secondary structure instability, and in vivo proteolysis; these problems severely compromise peptides as successful therapeutic agents [19]. In the present study, we applied the head-to-tail cyclization strategy to HBSP for improved stability and activity. Briefly, the peptide backbone was constrained via cyclization through main chain to main chain linkages, herein using thioether, (*R*)-sulfoxide, and (*S*)-sulfoxide connectors (Fig. 1A), which have been reported in our previous studies to achieve proteolytic resistance with activity retention or enhancement [7,8]. The synthetic procedures of cyclized peptides are shown in the Supplementary material (Fig. S1). Preliminary kidney IR injury assay indicated that the thioether-cyclized peptide (designated as CHBP) displayed a superior renoprotective effect to the sulfoxide versions. Therefore, the newly synthesized CHBP was chosen to evaluate in vitro and in vivo metabolic stabilities in comparison with the native linear peptide HBSP.

Since peptides are usually degraded mainly in the plasma by proteolysis, we prepared CHBP and HBSP in the human plasma at two different concentrations and analyzed the stability and half-life time using LC–MS/MS. As expected, HBSP was rapidly degraded in the human plasma at 0.2 and 1 μM, and the half-life time was 9.97 and 9.45 min, respectively (Fig. 1B and C). By contrast, CHBP was detected as 100% original peptide in the plasma during the experimental span of 300 min (Fig. 1D and E), indicating that the thioether-cyclized peptide CHBP was significantly stable in the human plasma. We also examined the stability of CHBP and HBSP in the cytochrome metabolism system using human hepatocytes. As shown in Fig. 1F and G, CHBP exhibited a 2.5-fold longer half-life than the corresponding linear peptide HBSP at the same concentration (Fig. 1F and G), suggesting that thioether cyclization protected the cyclic peptide CHBP from degradation by metabolic enzymes. Furthermore, CHBP also showed a remarkably slow metabolism in vivo (Fig. 1H). Taken together, we obtained a novel thioether-cyclized peptide CHBP, which was characterized by high resistance to proteolytic degradation and longer half-life time compared with HBSP.

3.2. CHBP stabilized the secondary structures of HBSP

To investigate whether cyclization affects the secondary structure of the cyclic peptide relative to the native peptide, we measured the CD spectra of the linear peptide HBSP and cyclized peptide CHBP. Two solvent systems were employed, namely, 40% acetonitrile (for solubility) in PBS buffer, and 50% trifluoroethanol (TFE) in PBS buffer. TFE is usually employed to induce the formation of the secondary structures of the peptide in aqueous solution. The observed positive maximum near 190 nm and double negative minima at 206 nm and 220 nm characterize an α-helix structure (Fig. S2, Table S1) [20]. The CD spectra suggested that the helix B surface peptide HBSP was apt to form α-helix, that thioether cyclization distinctly stabilized the α-helix geometry.

3.3. CHBP improved renal function and histological structure in the kidney IR injury model

To evaluate the renoprotective ability of CHBP, we analyzed the levels of blood urea nitrogen (BUN) and serum creatinine (Scr), which are two indicators of renal function. In a kidney ischemia and 48 h reperfusion murine model, CHBP treatment led to much lower levels of BUN and Scr compared with HBSP treatment (Fig. 2A and B). In a 7 d reperfusion murine model, BUN peaked at 48 h post-reperfusion, whereas the Scr level gradually increased until 48 h post-reperfusion and significantly decreased thereafter. These findings indicate that 48 h post-reperfusion marked the climax of kidney IR injury. CHBP administration at the onset of reperfusion dramatically reduced the levels of BUN and Scr at 6, 12, 24, and 48 h post-reperfusion (Fig. 2C and D). Renal histological assessment in each group was performed by H&E staining (Fig. 2E). Semi-quantitative analysis using a histological scoring system revealed that the tissue structure in the CHBP-treated group was well protected, with mild tubular dilation and interstitial edema, fewer protein casts in tubular lumens, and cellular infiltration, without tubular epithelial vacuolation or detachment frequently found in the CHBP-untreated group (Fig. 2F). In addition, we compared the in vivo renoprotective efficiency of CHBP with that of HBSP in a kidney ischemia and 15 d reperfusion murine model by extracellular matrix deposition examination. Both HBSP and CHBP were administered with only one dose (8 nmol/kg) at the onset of reperfusion. Extracellular matrix deposition in the kidney was evaluated by Sirius Red staining, which intercalated tertiary grooves in the structures of collagens I and III presented in pink under white light in the IR model. Sirius Red staining was mainly located in the tubulointerstitium, as shown by arrows (Fig. 2G). The CHBP group demonstrated significantly lowered staining compared with both the HBSP and IR groups in post-reperfusion kidneys (Fig. 2H).

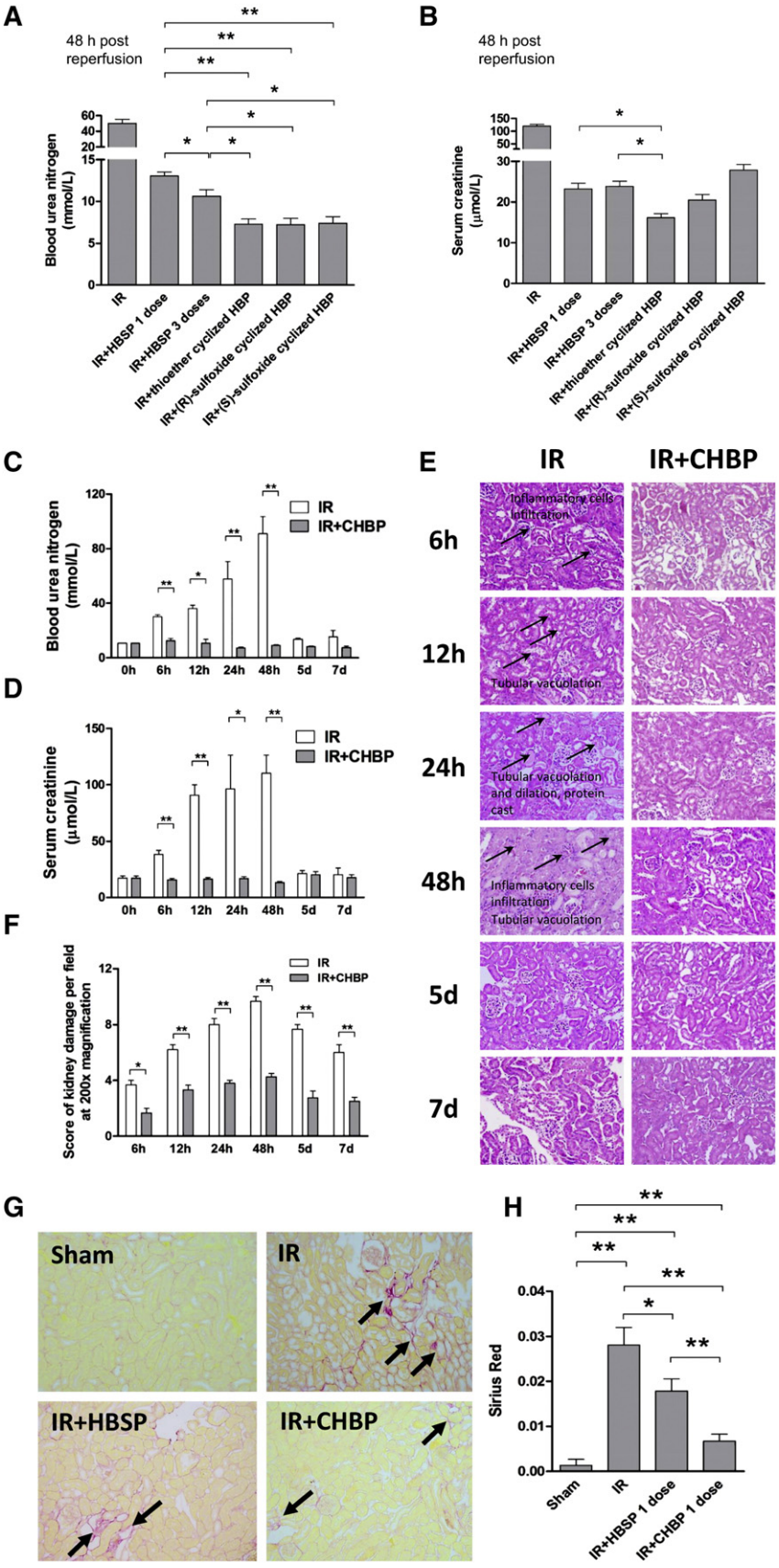

Fig. 2. Renal function in the screening of CHBP. In a kidney ischemia and 48 h reperfusion murine model, CHBP caused much lower levels of BUN and Scr compared with HBSP (A, B). In a 7 d reperfusion murine model, CHBP administration at the onset of reperfusion significantly reduced the levels of BUN and Scr at 6, 12, 24, and 48 h post-reperfusion (C, D). Moreover, CHBP significantly ameliorated renal histological injury detected by H&E staining (E, F). The in vivo renoprotective efficiency of CHBP was compared with that of HBSP in a kidney ischemia and 15 d reperfusion murine model by extracellular matrix deposition examination (G). The CHBP group demonstrated significantly lowered Sirius Red staining compared with both the HBSP and IR groups in post-reperfusion kidneys (H). Mean ± SD, $^{*}p < 0.05$; $^{**}p < 0.01$, n = 6.

3.4. CHBP ameliorated apoptosis in kidney IR injury

Considering that the protection of HBSP during kidney IR injury is mediated by two main processes: interference with apoptosis and inflammation, we detected them in the CHBP-treated IR model to explore the underlying mechanisms.

Apoptotic cells were determined by ISEL and active caspase-3 immunostaining in renal tissue sections (Fig. 3A and C). In the CHBP-treated group, ISEL + cells (Fig. 3B) and active caspase-3 + cells (Fig. 3D) were dramatically reduced in the kidney post-reperfusion.

3.5. CHBP decreased the inflammatory responses in kidney IR injury

MPO + neutrophils were detected by immunostaining to determine the effect of CHBP on inflammatory cell infiltration in the kidney (Fig. 4A). Most MPO + cells in the kidney were located in the vascular lumens and interstitial areas with polymorphic nucleus. MPO + cells gradually increased and peaked at 48 h post-reperfusion in the IR group, but significantly decreased in the CHBP-treated group at the corresponding time points (Fig. 4B). These findings suggest that CHBP significantly inhibited neutrophils recruited to the injured tissue, thereby prohibiting the inflammatory responses.

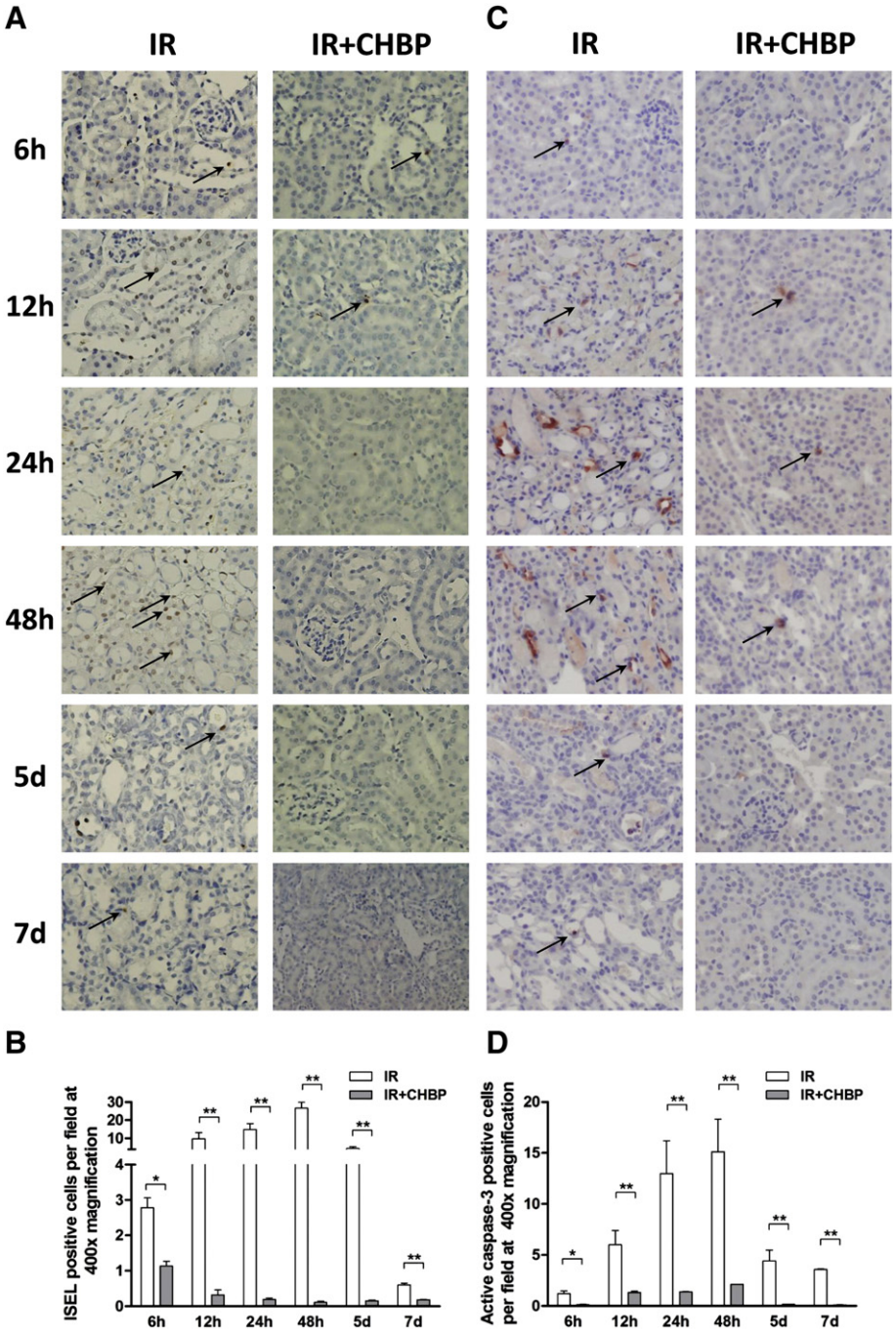

Fig. 3. Apoptotic cells in the kidney. ISEL + apoptotic cells were significantly decreased by CHBP post-reperfusion (A, B), as well as active caspase-3 + cells (C, D). Mean ± SD, $^{*}p < 0.05$; $^{**}p < 0.01$, n = 6.

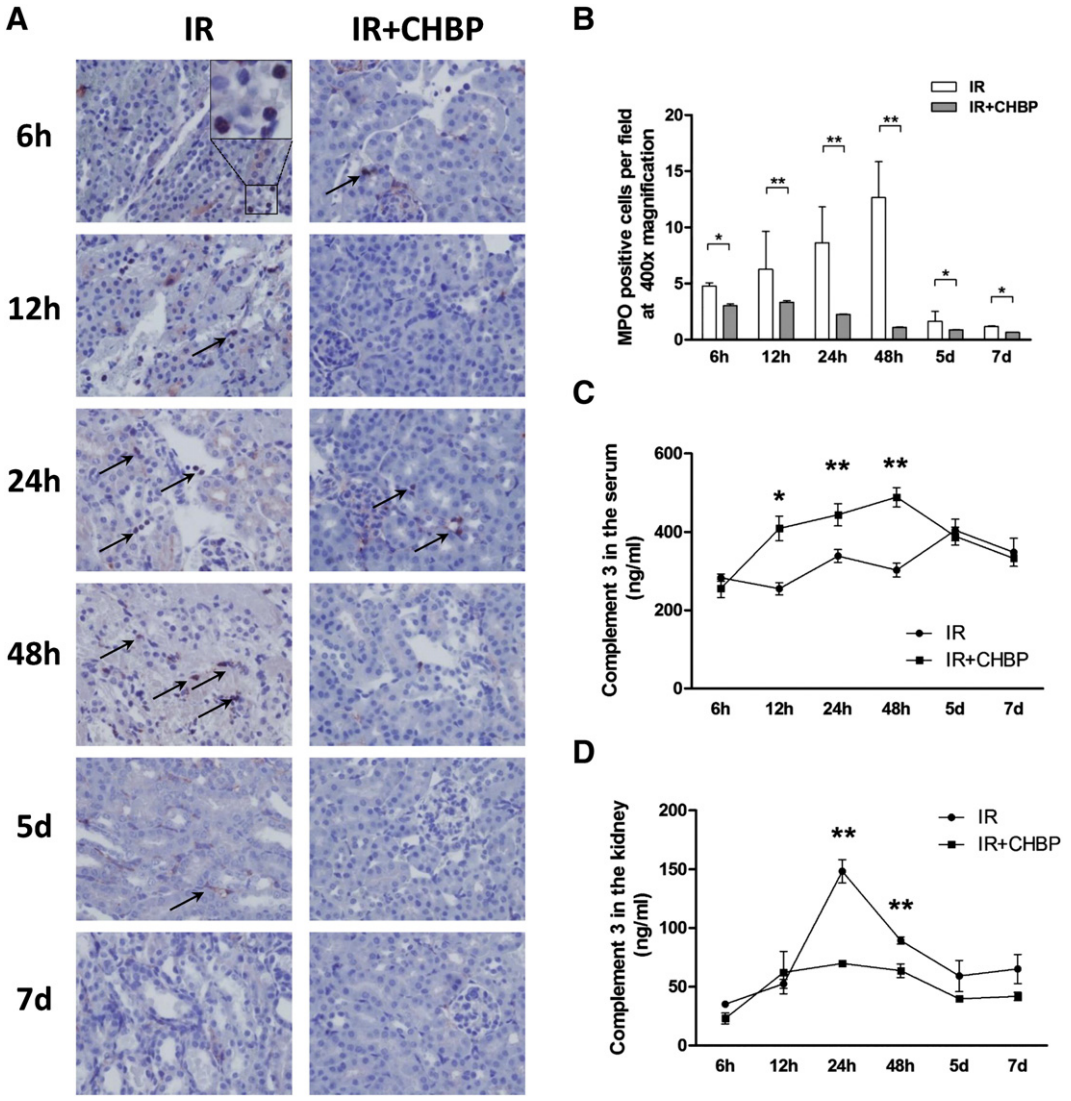

Fig. 4. Inflammatory responses in the kidney. MPO + cells were significantly reduced in the kidney by CHBP (A, B). In addition, the expression of C3 in the serum was significantly increased by CHBP at 12, 24, and 48 h post-reperfusion, indicating the ameliorated activation of C3. The expression of C3 in the kidney was significantly reduced at 24 and 48 h post-reperfusion in the CHBP-treated group, which revealed low local synthesis or deposition (C, D). Mean ± SD, $^{*}p < 0.05$; $^{**}p < 0.01$, n = 6.

The complement system actively regulates various steps of an inflammatory response. The activation of the complement system plays an important role in IR injury. The C3 level in both the serum and kidney was examined by ELISA. Compared with the CHBP-treated group, the expression of C3 in the serum significantly decreased in the IR group at 12, 24, and 48 h with increased expression in the kidney at 24 and 48 h-post reperfusion. These results indicate the activation of complement, and more deposition or local synthesis in the kidney (Fig. 4C and D).

We further determined the mRNA expression of inflammatory cytokine and transcription factors. In the CHBP-treated group, TNF-α was significantly decreased by 83%, 86%, and 93% at 6, 24, and 48 h post-reperfusion, respectively (Fig. 5A), and IL-6 was significantly decreased by 84%, 93%, and 85% at 6, 12, and 48 h post-reperfusion, respectively (Fig. 5B). The mRNA levels of cytokines and transcription factors of Treg and Th17 in the kidney were examined. IL-10 was remarkably upregulated at 6 h, 48 h, and 7 d post-reperfusion (Fig. 5C), and Foxp3 significantly increased at 6 h, 24 h, 48 h, and 5 d in the CHBP group (Fig. 5D). Furthermore, IL-17A and IL-17F, two important cytokines for Th17 cells, were significantly inhibited by CHBP (Fig. 5E and F), and RORγt significantly decreased at 12, 24, and 48 h post-reperfusion in the CHBP group (Fig. 5G).

3.6. CHBP induced autophagy in the IR-injured kidney

To elaborate signal transduction when treated with CHBP in the kidney IR injury model, antibody array was performed using kidney tissues at 48 h post-reperfusion (Fig. 6A). Interestingly, our results show that phosphorylated STAT3 and AMPKα significantly increased in the CHBP-treated group (Fig. 6B and C), and the phosphorylation of mTORC1 at S2448 significantly decreased (Fig. 6D). These proteins are related to autophagy [21,22].

Given that autophagy is demonstrated to be a renoprotective mechanism in IR injury, we also detected whether the renoprotective function of CHBP is mediated by autophagy. Our results depict a significant concurrent increase in the LC3-II/LC3-I ratio (autophagy) and beclin-1 in the CHBP-treated group (Fig. 7A–C), suggesting that CHBP might induce autophagy to exert its renoprotective functions. Considering that the mammalian target of rapamycin (mTOR) is a critical mediator of autophagy [23] and exists in two distinct complexes (i.e., mTORC1

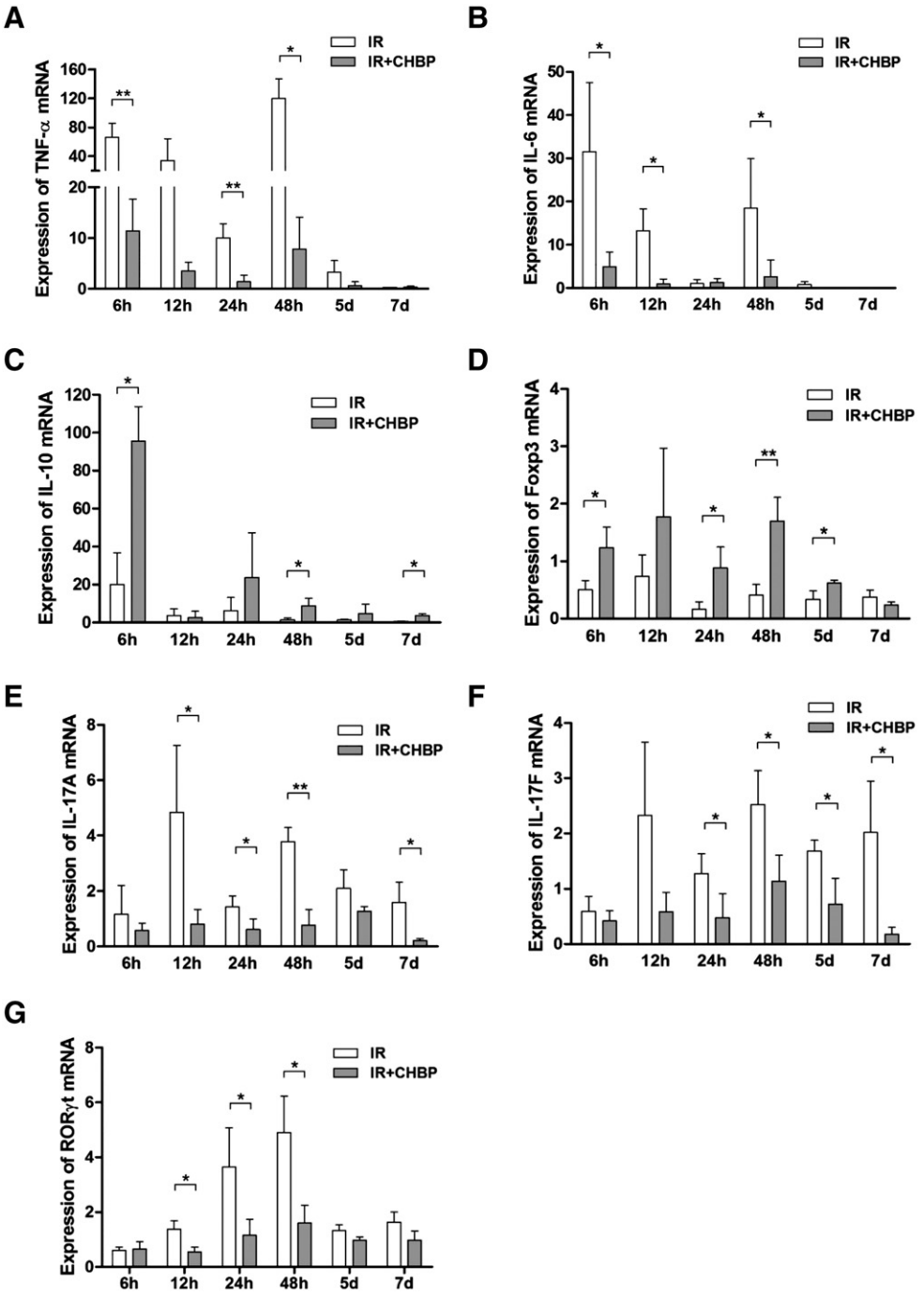

Fig. 5. CHBP modulated the mRNA expression of inflammatory cytokine and transcription factors. In the CHBP-treated group, TNF-α and IL-6 were significantly decreased at 6, 24, and 48 h post-reperfusion (A, B). IL-10 and Foxp3 were remarkably upregulated at 6 h, 48 h, and 7 d, or 6 h, 24 h, 48 h, and 5 d post-reperfusion, respectively (C, D). IL-17A, IL-17F, and RORγt were significantly inhibited by CHBP (E–G). Mean ± SD, $^{*}p < 0.05$; $^{**}p < 0.01$, n = 6.

and mTORC2), we evaluated the expression of mTORC after treatment with CHBP in the kidney IR model. Under CHBP treatment, mTOR complexes were differentially regulated in which the phosphorylation of mTORC1 at serine 2448 was inhibited, whereas the phosphorylation of mTORC2 at serine 2481 was increased (Fig. 7A, D, and E). Raptor, a component of mTORC1, was elevated by CHBP (Fig. 7A and F). Rictor, which is critical for mTORC2, was also increased by CHBP (Fig. 7A and G). To further analyze the role of mTORC1, we examined the activation of p70s6 kinase (phosphorylation at Thr389), a direct downstream target of mTORC1. Our results show that the p70s6 kinase was significantly reduced by CHBP treatment (Fig. 7A and H). Akt, the downstream target of mTORC2, was also activated via phosphorylation at serine 473 by Rictor (Fig. 7A and I). These results demonstrate, for the first time, that the novel CHBP could induce autophagy to exert renoprotective functions in the kidney IR model, and indicate that CHBP-induced autophagy was mainly through mTOR signaling.

In some conditions, autophagy is defined to be a cell survival mechanism that suppresses apoptosis. To further confirm the autophagy induction and anti-apoptotic effects of CHBP, we used an H_2O_2-induced renal TEC injury model in vitro. CHBP significantly inhibited apoptosis

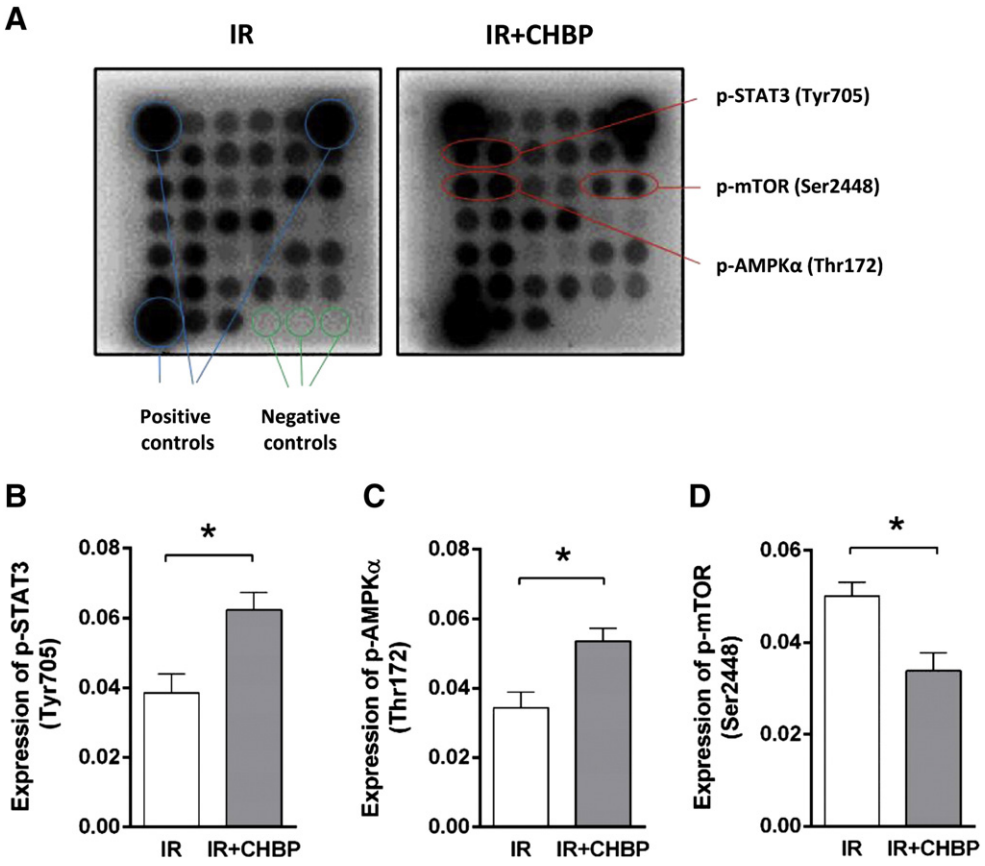

Fig. 6. Change in signal transduction induced by CHBP was screened by antibody array using kidney tissues at 48 h post-reperfusion (A). Phosphorylated STAT3 and AMPKα significantly increased in the CHBP-treated group (B, C), and the phosphorylation of mTORC1 at S2448 significantly reduced (D). The protein data were expressed as the corrected volume density against the mean volume density of three positive controls (blue circles) in the same well. Three dots at the bottom represent the negative controls (green circles) in the bottom right corner. Mean ± SD, $^{*}p < 0.05$; $^{**}p < 0.01$, n = 6.

and HBSP (Fig. 8A and B). In addition, CHBP revealed a stronger autophagy-inducing effect in terms of the higher expression of LC3-II/LC3-I (Fig. 8C). The in vitro experiment proved that CHBP could induce autophagy and suppress apoptosis.

4. Discussion

In this paper, we report for the first time a novel CHBP with improved metabolic stability and renoprotective potency. The functional motif of CHBP was derived from HBSP, but the peptide sequence was cyclized by a redox stable thioether linkage to gain proteolytic resistance and optimal geometric stabilization. CHBP demonstrated improved metabolic stability both in vitro (plasma and hepatocytes) and in vivo. Furthermore, some helicity was observed for linear peptide HBSP and the cyclization stabilized the α-helix structure of CHBP according to CD studies.

Given its short plasma half-life, linear HBSP needs to be frequently administered with high doses to achieve tissue-protective effects [24]. For example, in rodent peripheral nerve injury models, 30 μg/kg (23.5 nmol/kg) HBSP was administered five times i.p. at 2 d intervals, followed by once a week, showing reduced inflammation and long-term relief of allodynia [25]. In another murine nerve injury model, HBSP presented neural protective functions with a dose over tenfold of ours and five doses per week [26]. In addition, Brines et al. examined different doses of HBSP in a murine kidney IR injury model. They found that both 0.8 and 8 nmol/kg are most effective, but three administrations of HBSP are still needed [2]. For these deficiencies, the thioether-cyclized CHBP with constrained conformation confers a prolonged half-life time and enhanced potency to the cyclic peptide according to the mechanism of circular polypeptides [27]. The less extracellular matrix deposition in the post-reperfused kidney by CHBP compared with that by HBSP suggests that this long-acting CHBP could ameliorate IR injury with better outcomes, which benefited from its stability. In this study, only one dose of CHBP exerted persistent renal protection throughout the one week reperfusion injury in vivo.

In addition, for the first time, we identified CHBP-induced autophagy in the IR-injured kidney by upregulation of the LC3-II/I ratio and increased expression of beclin-1. HBSP has been demonstrated to be involved in the processes of apoptosis and inflammation. However, autophagy is defined to be a cell survival mechanism, and has been shown to be correlated with apoptosis and inflammation. Our results show that mTORC, which is the key regulator of autophagy [28], was consistently induced by CHBP. Furthermore, our study depicted possible signaling pathways, including mTOR regulation and AMPK activation, which link CHBP-induced autophagy with apoptosis and inflammatory responses. AMPK is a stress-activated kinase that acts to resort ATP levels back to homeostasis [29], and activation of AMPK plays an important role in protecting the kidney against IR injury [30]. In our study, the activated AMPK by CHBP suggests that CHBP promoted energy production through higher ATP levels under the condition of ATP depletion during IR injury. AMPK activates TSC2, which inhibits mTORC1 [31]. Moreover, CHBP treatment reduced phosphorylated mTOR (Ser2448) and p70s6 kinase (Thr389). These results suggest that the AMPK/mTORC1 pathway was involved in CHBP-mediated autophagy.

Interestingly, both AMPK and Akt are key regulators of kidney function and play critical roles in apoptosis [3,32]. However, potential crosstalk between the two under physiological or pathological conditions is unclear. According to our results, mTOR (mTORC1) was activated by Akt, but inhibited by AMPK via the phosphorylation of TSC2. Akt is also a downstream protein, which is phosphorylated at Ser473 by the activation of mTORC2. The convergence of the two at the level of mTOR

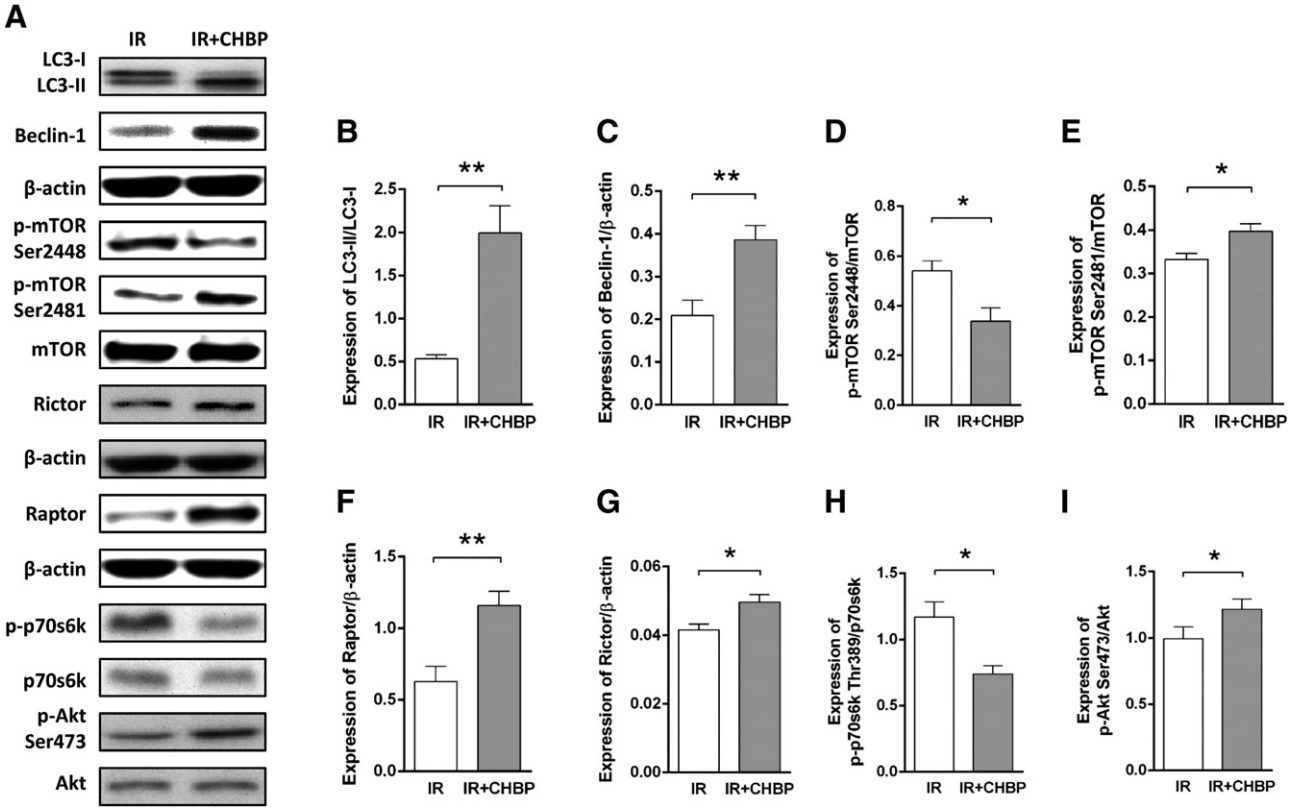

Fig. 7. CHBP-induced autophagy was determined by western blot in the IR-injured kidney (A). A significant concurrent increase was observed in the LC3-II/LC3-I ratio (autophagy) and beclin-1 in the CHBP-treated group (B, C). Under CHBP treatment, mTOR complexes were differentially regulated in which the phosphorylation of mTORC1 at serine 2448 was inhibited, whereas the phosphorylation of mTORC2 at serine 2481 increased (D, E). Raptor and Rictor were elevated by CHBP (F, G). The p70s6 kinase (phosphorylation at Thr389), a direct downstream target of mTORC1, was significantly reduced by CHBP treatment (H). Akt, the downstream target of mTORC2, was also activated via phosphorylation at serine 473 (I). Mean ± SD, $^{*}p < 0.05$; $^{**}p < 0.01$, n = 6.

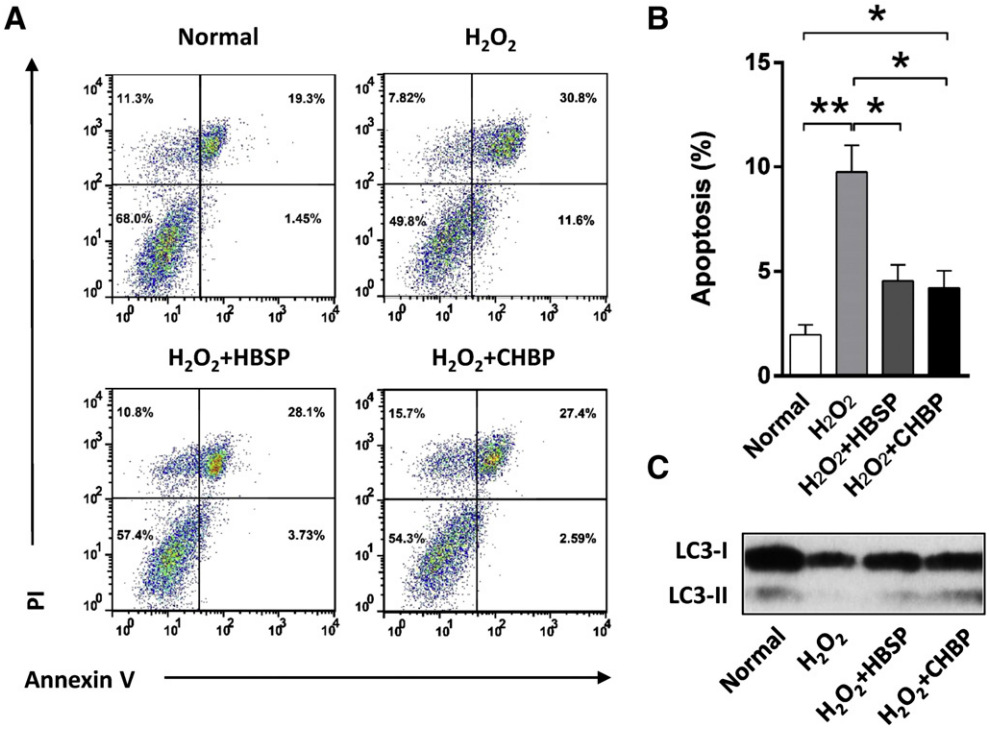

Fig. 8. CHBP protected renal TECs against H_2O_2-induced apoptosis and promoted autophagy. CHBP and HBSP significantly inhibited apoptosis of renal TECs (A, B). However, CHBP revealed a stronger autophagy-inducing effect in terms of the higher expression of LC3-II/LC3-I (C). Mean ± SD, $^{*}p < 0.05$; $^{**}p < 0.01$, n = 6.

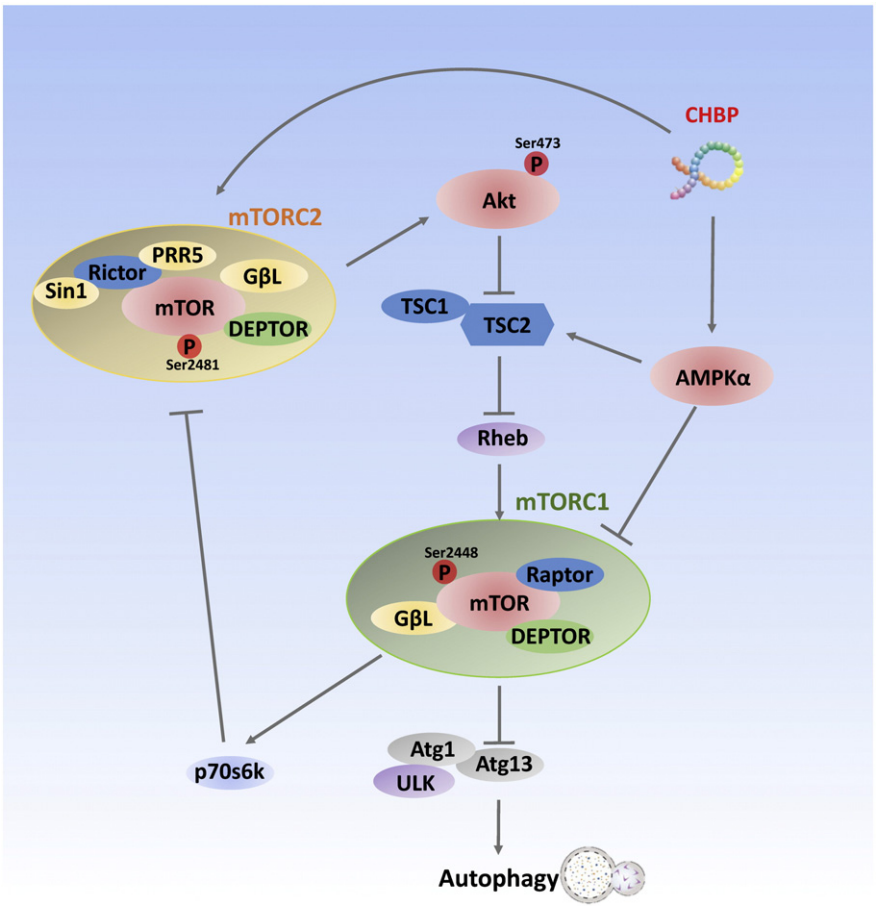

Fig. 9. Schematic illustration of the pathway mediated by CHBP. CHBP-induced autophagy is mediated by inhibition of mTORC1 and activation of mTORC2.

may serve as a critical avenue for the crosstalk between AMPK and Akt during pathophysiological adaption. Consequently, CHBP activated mTORC2–Akt and inhibited mTORC1 by activating AMPK (Fig. 9). However, the precise regulatory mechanism between mTORC1 and mTORC2 needs further investigation.

Indeed, autophagy plays key roles in the immune systems [33]. In our study, CHBP significantly upregulated the mRNA expression of Foxp3 and IL-10, suggesting an increase in Treg and promoted immunoregulation by CHBP in kidney IR injury. IL-17A and IL-17F initiate inflammatory responses by increasing the expression of pro-inflammatory cytokines and chemokines, regulating neutrophil infiltration [34], which was significantly reduced by CHBP, decreasing neutrophil infiltration, and alleviating kidney histological lesions. RORγt was also remarkably reduced in the kidney by CHBP at the peak of IR injury. Therefore, CHBP upregulated Treg and inhibited Th17 in the kidney during IR injury to modulate the adaptive immunity in terms of restoring the Treg/Th17 balance.

We screened signaling proteins in the kidney at 48 h post-reperfusion when the injury reached its peak. The results reveal that CHBP activated STAT3 and AMPKα, but inhibited mTOR. The activation of STAT3 protects the liver and heart against IR injury [35,36], and inhibition of apoptosis is one of its mechanisms in ATP depletion/recovery-induced TEC injury model [37]. In the CHBP-treated group, enhanced STAT3 phosphorylation and decreased apoptotic cells were observed in the kidney, indicating that CHBP suppressed apoptosis via STAT3 pathway activation.

In conclusion, the novel thioether-cyclized peptide CHBP demonstrated much better stability than HBSP with less dose but longer and stronger action both in vitro and in vivo. We proposed a potential signaling pathway in which CHBP-induced autophagy in response to IR via inhibition of mTORC1 and activation of mTOR2 was closely related to decreasing inflammation and apoptosis. This study suggested not only the metabolically stable CHBP as a promising new therapy for the treatment of kidney IR injury, but also the pivotal role of the AMPK/Akt/mTOR signaling cascade in autophagy regulation of CHBP-mediated renoprotection.

Supplementary data to this article can be found online at http://dx.doi.org/10.1016/j.bbadis.2014.09.001.

Conflicts of interest

The authors declare no conflict of interest.

Acknowledgements

This study was supported by the National Natural Science Foundation of China (81270832, 81270833, 81021062, 81370852, 81123004, 81400752 and 21302201) and the Science and Technology Commission of Shanghai Municipality (12ZR1405500, 13ZR1447700). We also thank Ms. Jianying Shi at the Department of Pathophysiology, Shanghai Medical College, Fudan University for help with histological assessment.

References

[1] L. Velly, L. Pellegrini, B. Guillet, N. Bruder, P. Pisano, Erythropoietin 2nd cerebral protection after acute injuries: a double-edged sword? Pharmacol. Ther. 128 (2010) 445–459.
[2] M. Brines, N.S. Patel, P. Villa, C. Brines, T. Mennini, M. De Paola, Z. Erbayraktar, S. Erbayraktar, B. Sepodes, C. Thiemermann, P. Ghezzi, M. Yamin, C.C. Hand, Q.W. Xie, T. Coleman, A. Cerami, Nonerythropoietic, tissue-protective peptides derived from the tertiary structure of erythropoietin, Proc. Natl. Acad. Sci. U. S. A. 105 (2008) 10925–10930.
[3] C. Yang, T. Zhao, M. Lin, Z. Zhao, L. Hu, Y. Jia, Y. Xue, M. Xu, Q. Tang, B. Yang, R. Rong, T. Zhu, Helix B surface peptide administered after insult of ischemia reperfusion improved

renal function, structure and apoptosis through beta common receptor/erythropoietin receptor and PI3K/Akt pathway in a murine model, Exp. Biol. Med. (Maywood) 238 (2013) 111–119.
[4] W.G. van Rijt, G.J. Nieuwenhuijs-Moeke, H. van Goor, B. Jespersen, P.J. Ottens, R.J. Ploeg, H.G. Leuvenink, ARA290, a non-erythropoietic EPO derivative, attenuates renal ischemia/reperfusion injury, J. Transl. Med. 11 (2013) 9.
[5] M. Brines, A. Cerami, The receptor that tames the innate immune response, Mol. Med. 18 (2012) 486–496.
[6] Y.Q. Long, R. Guo, J.H. Luo, D. Yang, P.P. Roller, Potentiating effect of distant sites in non-phosphorylated cyclic peptide antagonists of the Grb2-SH2 domain, Biochem. Biophys. Res. Commun. 310 (2003) 334–340.
[7] Y.L. Song, M.L. Peach, P.P. Roller, S. Qiu, S. Wang, Y.Q. Long, Discovery of a novel nonphosphorylated pentapeptide motif displaying high affinity for Grb2-SH2 domain by the utilization of 3′-substituted tyrosine derivatives, J. Med. Chem. 49 (2006) 1585–1596.
[8] Y.Q. Long, T. Xue, Y.L. Song, Z.L. Liu, S.X. Huang, Q. Yu, Synthesis and utilization of chiral alpha-methylated alpha-amino acids with a carboxyalkyl side chain in the design of novel Grb2-SH2 peptide inhibitors free of phosphotyrosine, J. Med. Chem. 51 (2008) 6371–6380.
[9] G.R. Kinsey, R. Sharma, L. Huang, L. Li, A.L. Vergis, H. Ye, S.T. Ju, M.D. Okusa, Regulatory T cells suppress innate immunity in kidney ischemia–reperfusion injury, J. Am. Soc. Nephrol. 20 (2009) 1744–1753.
[10] B. Yang, S. Jain, I.Z. Pawluczyk, S. Imtiaz, L. Bowley, S.Y. Ashra, M.L. Nicholson, Inflammation and caspase activation in long-term renal ischemia/reperfusion injury and immunosuppression in rats, Kidney Int. 68 (2005) 2050–2067.
[11] J. Yang, H.N. Ahn, M. Chang, P. Narasimhan, P.H. Chan, Y.S. Song, Complement component 3 inhibition by an antioxidant is neuroprotective after cerebral ischemia and reperfusion in mice, J. Neurochem. 124 (2013) 523–535.
[12] D. Hanidziar, M. Koulmanda, Inflammation and the balance of Treg and Th17 cells in transplant rejection and tolerance, Curr. Opin. Organ Transplant. 15 (2010) 411–415.
[13] Z. Wang, M.E. Choi, Autophagy in kidney health and disease, Antioxid. Redox Signal. 20 (2014) 519–537.
[14] G.P. Kaushal, Autophagy protects proximal tubular cells from injury and apoptosis, Kidney Int. 82 (2012) 1250–1253.
[15] M.H. Zou, Z. Xie, Regulation of interplay between autophagy and apoptosis in the diabetic heart: new role of AMPK, Autophagy 9 (2013) 624–625.
[16] H. Ueba, M. Brines, M. Yamin, T. Umemoto, J. Ako, S. Momomura, A. Cerami, M. Kawakami, Cardioprotection by a nonerythropoietic, tissue-protective peptide mimicking the 3D structure of erythropoietin, Proc. Natl. Acad. Sci. U. S. A. 107 (2010) 14357–14362.
[17] Z. Zhao, C. Yang, L. Wang, L. Li, T. Zhao, L. Hu, R. Rong, M. Xu, T. Zhu, The regulatory T cell effector soluble fibrinogen-like protein 2 induces tubular epithelial cell apoptosis in renal transplantation, Exp. Biol. Med. (Maywood) 239 (2014) 193–201.
[18] C. Yang, Y. Jia, T. Zhao, Y. Xue, Z. Zhao, J. Zhang, J. Wang, X. Wang, Y. Qiu, M. Lin, D. Zhu, G. Qi, Q. Tang, R. Rong, M. Xu, S. Ni, B. Lai, M.L. Nicholson, T. Zhu, B. Yang, Naked caspase 3 small interfering RNA is effective in cold preservation but not in autotransplantation of porcine kidneys, J. Surg. Res. 181 (2013) 342–354.
[19] P. Li, P.P. Roller, Cyclization strategies in peptide derived drug design, Curr. Top. Med. Chem. 2 (2002) 325–341.
[20] N.E. Shepherd, H.N. Hoang, G. Abbenante, D.P. Fairlie, Single turn peptide alpha helices with exceptional stability in water, J. Am. Chem. Soc. 127 (2005) 2974–2983.
[21] J.W. Lee, S. Park, Y. Takahashi, H.G. Wang, The association of AMPK with ULK1 regulates autophagy, PLoS One 5 (2010) e15394.
[22] T. Yokoyama, Y. Kondo, S. Kondo, Roles of mTOR and STAT3 in autophagy induced by telomere 3′ overhang-specific DNA oligonucleotides, Autophagy 3 (2007) 496–498.
[23] P. Codogno, A.J. Meijer, Autophagy and signaling: their role in cell survival and cell death, Cell Death Differ. 12 (2005) 1509–1518.
[24] C.M. McVicar, R. Hamilton, L.M. Colhoun, T.A. Gardiner, M. Brines, A. Cerami, A.W. Stitt, Intervention with an erythropoietin-derived peptide protects against neuroglial and vascular degeneration during diabetic retinopathy, Diabetes 60 (2011) 2995–3005.
[25] M. Swartjes, A. Morariu, M. Niesters, M. Brines, A. Cerami, L. Aarts, A. Dahan, ARA290, a peptide derived from the tertiary structure of erythropoietin, produces long-term relief of neuropathic pain: an experimental study in rats and beta-common receptor knockout mice, Anesthesiology 115 (2011) 1084–1092.
[26] R.E. Schmidt, D. Feng, Q. Wang, K.G. Green, L.L. Snipes, M. Yamin, M. Brines, Effect of insulin and an erythropoietin-derived peptide (ARA290) on established neuritic dystrophy and neuronopathy in Akita (Ins2 Akita) diabetic mouse sympathetic ganglia, Exp. Neurol. 232 (2011) 126–135.
[27] T.L. Aboye, J.A. Camarero, Biological synthesis of circular polypeptides, J. Biol. Chem. 287 (2012) 27026–27032.
[28] Y. Suh, F. Afaq, N. Khan, J.J. Johnson, F.H. Khusro, H. Mukhtar, Fisetin induces autophagic cell death through suppression of mTOR signaling pathway in prostate cancer cells, Carcinogenesis 31 (2010) 1424–1433.
[29] Y.J. Ahn, H. Kim, H. Lim, M. Lee, Y. Kang, S. Moon, H.S. Kim, H.H. Kim, AMP-activated protein kinase: implications on ischemic diseases, BMB Rep. 45 (2012) 489–495.
[30] P.W. Seo-Mayer, G. Thulin, L. Zhang, D.S. Alves, T. Ardito, M. Kashgarian, M.J. Caplan, Preactivation of AMPK by metformin may ameliorate the epithelial cell damage caused by renal ischemia, Am. J. Physiol. Renal Physiol. 301 (2011) F1346–F1357.
[31] H. Takagi, Y. Matsui, S. Hirotani, H. Sakoda, T. Asano, J. Sadoshima, AMPK mediates autophagy during myocardial ischemia in vivo, Autophagy 3 (2007) 405–407.
[32] N.M. Pastor-Soler, K.R. Hallows, AMP-activated protein kinase regulation of kidney tubular transport, Curr. Opin. Nephrol. Hypertens. 21 (2012) 523–533.
[33] K. Watanabe, T. Tsubata, Autophagy connects antigen receptor signaling to costimulatory signaling in B lymphocytes, Autophagy 5 (2009) 108–110.
[34] H. Kono, H. Fujii, M. Ogiku, N. Hosomura, H. Amemiya, M. Tsuchiya, M. Hara, Role of IL-17A in neutrophil recruitment and hepatic injury after warm ischemia–reperfusion mice, J. Immunol. 187 (2011) 4818–4825.
[35] S. Suzuki, K. Inaba, H. Konno, Ischemic preconditioning in hepatic ischemia and reperfusion, Curr. Opin. Organ Transplant. 13 (2008) 142–147.
[36] H.F. Luan, Z.B. Zhao, Q.H. Zhao, P. Zhu, M.Y. Xiu, Y. Ji, Hydrogen sulfide postconditioning protects isolated rat hearts against ischemia and reperfusion injury mediated by the JAK2/STAT3 survival pathway, Braz. J. Med. Biol. Res. 45 (2012) 898–905.
[37] J. Wang, C. Ouyang, X. Chen, B. Fu, Y. Lu, Q. Hong, STAT3 inhibits apoptosis of human renal tubular epithelial cells induced by ATP depletion/recovery, Nephron Exp. Nephrol. 108 (2008) e11–e18.